REVIEW

Single-Molecule Biomechanics with Optical Methods

Amit D. Mehta,[1] Matthias Rief,[1] James A. Spudich,[1]*
David A. Smith,[2] Robert M. Simmons[2]*

Single-molecule observation and manipulation have come of age. With the advent of optical tweezers and other methods for probing and imaging single molecules, investigators have circumvented the model-dependent extrapolation from ensemble assays that has been the hallmark of classical biochemistry and biophysics. In recent years, there have been important advances in the understanding of how motor proteins work. The range of these technologies has also started to expand into areas such as DNA transcription and protein folding. Here, recent experiments with rotary motors, linear motors, RNA polymerase, and titin are described.

A new era of biomechanical studies has been ushered in by the development of optical and mechanical probes that are sensitive enough to make measurements on single biological molecules. Not only do such measurements throw light on well-characterized molecules, but they make it possible to investigate the properties of molecules whose role and function are unknown. A general goal in molecular biophysics is to characterize mechanistically the behavior of single molecules. Whereas past experiments required model-dependent inferences from ensemble measurements, these new techniques allow a direct observation of the parameters that are relevant to answering the following questions: How does a protein move? How does it generate force? How does it respond to applied force? How does it unfold?

Not surprisingly, the initial applications of the new techniques involved molecules that produce active movement against load (for example, "molecular motors" such as myosin, which drives muscle contraction). A number of "molecular machines" (for instance, DNA-processing enzymes) are now accessible to single-molecule observation and manipulation. Among other obvious targets were more passive molecules (such as biopolymers) that respond to an applied force in various ways. This field was initially developed by work on DNA, but more recently, it has been extended to structural biopolymers. In the past 6 years, observations of molecular motors and biopolymers have included the following: stepwise motion of single kinesin molecules along a microtubule track, displacement of an actin filament by a single myosin molecule, forces and transcriptional pauses associated with RNA polymerase activity, nonlinear elasticity of single polymers, reversible unfolding of single-protein domains by applied force, and discrete rotations of a single F_1 subunit of the F_0F_1–adenosine triphosphate (ATP) synthase. The parallel development of single-fluorophore detection has allowed these mechanical measurements to be combined with observations of substrate binding, protein position, and conformational change. Here, we mainly focus on the use of optical trapping technology, including the rival techniques of glass microneedles and atomic force microscopes (AFMs) where appropriate.

Optical Tweezers Technique

Optical tweezers, or optical traps (*1*), exploit the fact that light exerts force on matter. Dielectric particles, such as uniform beads or bacterial cells, are attracted to and trapped near the waist of a laser beam that has been focused through a microscope objective. Applied external forces will displace a trapped bead from the trap center, with a linear dependence of displacement on force. Such traps can be made sufficiently compliant so that they exert little resistance to the movement produced by single molecules.

Biological macromolecules can be bound to polystyrene or silica beads, which are usually ~1 μm in diameter. A trap can then be moved to steer a bead into a desired experimental geometry (for example, to interact with a partner molecule attached to a coverslip). Upon binding between the two molecules, the forces and movements involved can be measured, and the interaction can be perturbed by moving the trap. Similar experiments can be performed with glass microneedles or AFMs, although such probes are typically less compliant than optical ones. Only the most compliant probes will yield to forces generated by single molecules, rendering them visible.

Rotary Motors: The Bacterial Flagella Motor and the F_1–Adenosine Triphosphatase (ATPase)

Motile bacteria, such as *Escherichia coli*, are propelled by the rotation of a number of flagella that are several micrometers long. Each flagellum has a membrane-bound rotary motor at its base, consisting of a rotor with ~30-fold symmetry and a stator (the section of the motor that does not rotate) with eight independent molecular motors. Each molecular motor is powered by a proton (or, in some cases, a sodium ion) gradient. In one of the first quantitative applications of optical tweezers, Block *et al.* (*2*) measured the nonlinear torsional elasticity of the link between the flagellum and the motor by trapping the cell body of a bacterium whose flagellum was fixed to a coverslip.

More recently, Noji *et al.* (*3*) have identified the F_1-ATPase as a rotary motor. The F_0F_1-ATP synthase (see Fig. 1A) is a multidomain complex consisting of two units: a hydrophobic proton channel (F_0) embedded in the mitochondrial membrane and a hydrophilic catalytic unit (F_1) protruding into the mitochondria, converting adenosine diphosphate (ADP) to ATP (*4*). The complex can be thought of as two rotary motor units coupled together mechanically. The F_1F_0-ATP synthase is reversible; whereas the full enzyme complex can synthesize or hydrolyze ATP, F_1 in isolation only hydrolyzes it. Rotation of F_1 had been long suspected (*5*), but it was demonstrated only recently by directly observing the motion of a fluorescent actin filament specifically bound to the rotor element (Fig. 1B) (*3*). Yasuda *et al.* (*6*) observed this rotation under low ATP concentrations and with actin filaments of variable length. As anticipated from the threefold rotational symmetry of F_1 (*5*), they observed discrete 120° rotations (see Fig. 1C). These were coupled tightly to ATP binding events, as judged by the distribution of dwell times separating the angular rotations. Moreover, they estimated the work required to rotate the actin filament against viscous load to be as much as 80 pN·nm, which is approximately the free energy liberated by a single ATP hydrolysis under physiological conditions. From this estimate, they concluded that the F_1-ATPase can couple nearly 100% of its ATP-derived energy into mechanical work. In this respect, it appears that nature has far outperformed

[1]Department of Biochemistry B400, Stanford University School of Medicine, Stanford, CA 94305–5307, USA. [2]Randall Institute, King's College London, 26–29 Drury Lane, London WC2B 5RL, UK.

*To whom correspondence should be addressed.

human engineers, making mechanistic understanding of these extraordinarily efficient motors an important goal.

Whereas structural, mechanical, and kinetic studies have merged to form a coherent picture of the F_1-ATPase, the F_0 subunit still awaits a similar understanding. F_0 is mechanically linked to the γ domain (Fig. 1A) and is powered by an ion channel. It remains to be demonstrated if F_0 rotates in isolation and if the F_1 and F_0 subunits in a complex each rotate in relation to the other.

Kinesin: Vesicle Transport Along Microtubules

The most intensive applications of optical tweezers have been focused on linear motor proteins, which move along a polymer track. The two-headed dimer kinesin transports vesicles along microtubules (hollow tubes formed from tubulin dimers), a key component of the cellular cytoskeleton. Kinesin is an example of a processive motor protein, which can undergo multiple productive catalytic cycles per diffusional encounter with its track. Processive motors must have a high duty ratio, or fraction of turnover time when a head is strongly bound with the track (*7, 8*). A single kinesin molecule can move along a microtubule for several micrometers before dissociating (*9, 10*). Vale *et al.* (*11*) have imaged single fluorophores bound to kinesin molecules and have observed similar distances traversed by single molecules before they release from the microtubule.

To characterize its motion at a high spatial resolution, Svoboda *et al.* (*12*) attached kinesin at low density to silica beads, trapped a bead, and moved it near a microtubule that was fixed on a microscope coverslip (Fig. 2A). The kinesin advanced in discrete steps of 8 nm [the tubulin repeat unit on the microtubule track (Fig. 2B)], which were clearly distinguished from Brownian motion at low ATP concentration or at high load. The steps were separated by dwell periods of variable length (*12*). The kinesin moved the bead away from the trap center, slowed as the resistive force increased, and finally stalled under loads of 5 pN, although Kojima *et al.* have observed stall forces up to 7 pN (*13*). The kinesin stepped backward occasionally near stalling conditions, but it did not step backward continuously in response to increased load against the direction of movement (*14*). The rate of movement slowed linearly with increasing force over a broad range of ATP concentrations (*13, 15, 16*). If load affects one or more biochemical rate constants, one would expect the shape of this force-velocity curve to differ between the high- and low-ATP cases. From the linear shape of these curves under all ATP conditions, Svoboda and Block (*15*) and Meyhöfer and Howard (*16*) argued that load does not affect the catalysis rate but instead decreases the probability of a catalytic cycle producing a mechanical step.

To elucidate the kinetic scheme underlying the 8-nm advances, several investigators have analyzed the distribution of dwell times between steps. Particularly at low ATP concentrations, it is possible to determine if each step follows one or two ATP binding events or if two steps follow one such event (*17*). However, the relevant distributions of dwell periods differ most when the dwell times are shortest and thus when the adjacent steps are hardest to separate. Kojima *et al.* (*13*) tried to identify enough steps to fit the distribution, whereas Hua *et al.* (*18*) incorporated the probability of missing fast ones. Both concluded that one rate-limiting process, ATP binding, precedes every 8-nm advance. Schnitzer and Block (*19*) reached the same conclusion by analyzing variations within an ensemble of staircaselike displacement data using a method of fluctuation analysis (*20*), which does not depend on observing the steps directly. Therefore, unlike in the case of myosin, loosely coupled kinesin models no longer find support.

Such measurements eliminate models that postulate two ATP-dependent head movements producing each 8-nm step, suggesting instead that kinesin may work through 16-nm hand-over-hand movements of the two heads (Fig. 2C, left and middle), with each step advancing the center of the molecule by 8 nm (*21*). It is difficult to reconcile such large movements with the compact structure of the dimer, although it is conceivable that part of the molecule unfolds to accommodate them. Although the coiled-coil region separating the heads seemed a likely candidate for such unfolding (*22*), a recent study demonstrated that unfolding in this region is not necessary for kinesin to move processively (*23*). Alternatively, each 8-nm step may involve a cooperative movement with one head dragging the other, limping rather than walking (Fig.

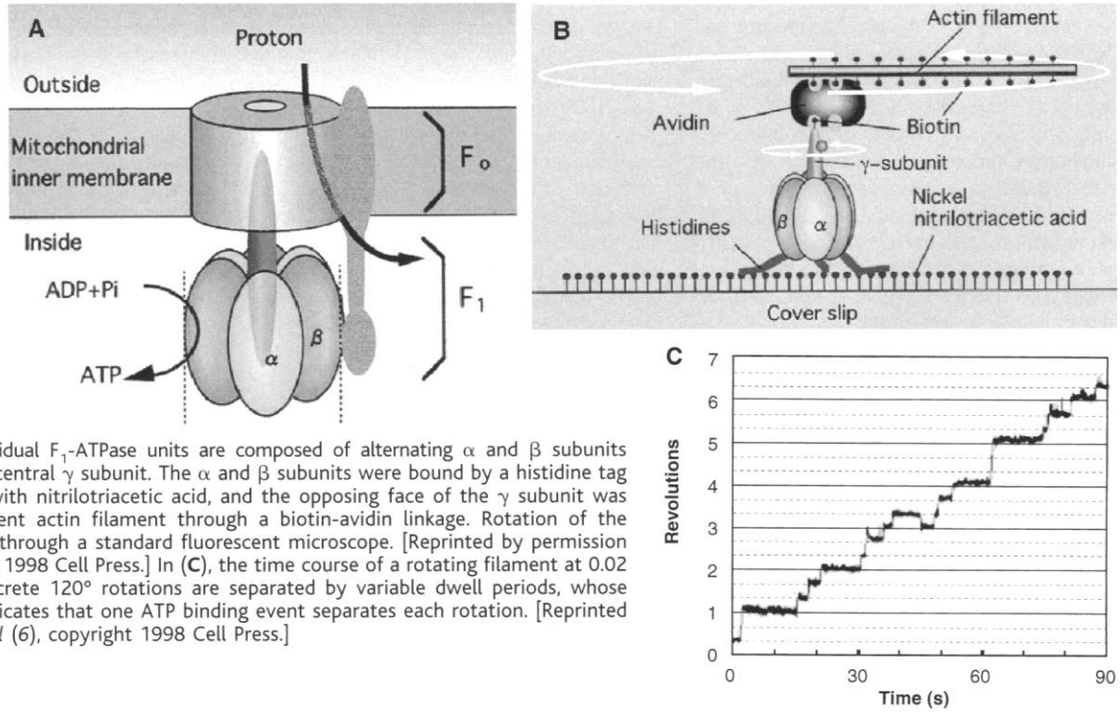

Fig. 1. (**A**) Schematic diagram of the F_0F_1-ATP synthase. The hydrophobic F_0 subunit is embedded in the mitochondrial membrane, whereas the hydrophilic F_1 unit, which has been demonstrated to rotate, projects into the mitochondria. [Reprinted by permission from *Cell* (*4*), copyright 1998 Cell Press.] (**B**) Experimental geometry used by Noji *et al.* (*3*) to observe the rotation of single F_1-ATPase molecules. Individual F_1-ATPase units are composed of alternating α and β subunits surrounding a rotating central γ subunit. The α and β subunits were bound by a histidine tag to a coverslip coated with nitrilotriacetic acid, and the opposing face of the γ subunit was attached to a fluorescent actin filament through a biotin-avidin linkage. Rotation of the filament was observed through a standard fluorescent microscope. [Reprinted by permission from *Cell* (*4*), copyright 1998 Cell Press.] In (**C**), the time course of a rotating filament at 0.02 μM ATP is shown. Discrete 120° rotations are separated by variable dwell periods, whose Poisson distribution indicates that one ATP binding event separates each rotation. [Reprinted by permission from *Cell* (*6*), copyright 1998 Cell Press.]

2C, right). These models may predict limited processivity from a single kinesin head. Studies of single-headed kinesin constructs should further clarify these possibilities; studies to date indicate that sustained movement is observed only when more than one single-headed kinesin molecule is involved in an interaction (*24–27*), indicating that both heads are required for processive motion by a single molecule.

Single-molecule studies of kinesin, coupled with recent structural advances, have substantially progressed in narrowing the range of accepted models that can account for processive movement. However, little detail has emerged about the nature of the mechanical step itself. The similarity between the structures of myosin and kinesin suggests that kinesin must undergo a conformational change at some point during its kinetic cycle, which also suggests intermediate step sizes. However, it remains difficult to imagine a large conformational change from such a small molecule, which lacks a visible "lever arm." Controlled movements at higher forces may be a more promising route. Visscher and Block (*28*) have recently developed a trap that is capable of exerting a fixed force on a moving bead by maintaining a constant bead-trap separation; this should also enable more precise studies of mechanochemical coupling.

Myosin: The Muscle Motor

Myosin II (skeletal muscle myosin) is a linear two-headed motor that interacts with actin filaments, which are helical polymers found in muscle thin filaments and in the cytoskeleton. Aside from muscle contraction, myosin II is also involved in several forms of cell movement, including cell shape changes, cytokinesis, capping of cell surface receptors, and retraction of pseudopods (*29*). Myosin II shares many structural features with kinesin (*30*). Both use ATP to move along their respective tracks, but myosin II is nonprocessive—it undergoes (at most) one catalytic cycle per diffusional encounter with its track (*7, 31*). Although this means that a single molecule cannot move along its track for large distances, it also means that organized ensembles of molecules can move their track at higher speeds. Myosin is thought to undergo a conformational change when it binds to actin, resulting in a "working stroke." For the coupling of such transient interactions and movements to a trapped bead, a more complex geometry is needed than that described above for kinesin. Finer *et al.* (*32*) formed a "dumbbell" structure of an actin filament bound at either end to a polystyrene bead. They trapped both beads, pulled the filament taut, and moved it near surface-bound silica spheres that were decorated sparsely with myosin molecules (Fig. 3A). They observed transient bead deflections parallel to the long filament axis and interpreted these as reflecting myosin binding and pulling the filament. Unlike kinesin, at low density, myosin II moved the filament only once upon binding and then released it after a variable dwell period. Myosin release follows ATP binding, and therefore, Finer *et al.* extended the duration of binding events by lowering the ATP concentration to make the events more distinct in relation to the thermal noise. In filtered data, they observed pronounced bead deflections that were centered around 11 nm, dependence of event duration on ATP concentration, and load-dependent dissociation rates. These experiments could not resolve a number of issues regarding the magnitude of the working stroke (or step size). These include the following: the thermal diffusion (Brownian motion) of the actin-bead dumbbell, the compliance between the actin and bead, the question of whether all binding events were detected, the relative orientation of the myosin and actin filament, the nonspecific mounting of myosin to the surface, and the role of the two myosin heads. These and other issues were confronted by the work that followed.

Thermal diffusion complicates the task of measuring the myosin step size. At the weak trap strengths that are required to minimize the load confronting myosin, a dumbbell undergoes diffusion over ~50 nm, which is much higher than the step size. Thus, a myosin molecule will often face actin sites that have been already offset from the baseline center, making the observed dumbbell displacement by myosin the sum of its initial thermal offset and the distance by which myosin moves it. The distribution of such displacements therefore resembles in shape and size (but shifted upward by the step distance) the spread of bead position at the baseline (*33*). In the absence of ATP, the distribution of bead movements induced by myosin binding was similar to this but centered around 0 nm, indicating no net displacement (*34*). These studies did not use the bead displacement but instead used the increase in stiffness constraining bead diffusion (seen as a decrease in diffusion amplitude) as a signature of myosin binding. This allowed the identification of small displacements that were difficult to see in filtered bead position data.

Optical trapping studies of myosin suggest a step size of 4 to 15 nm (*32–37*). In most of these studies, the surface-bound myosins were aligned randomly with respect to

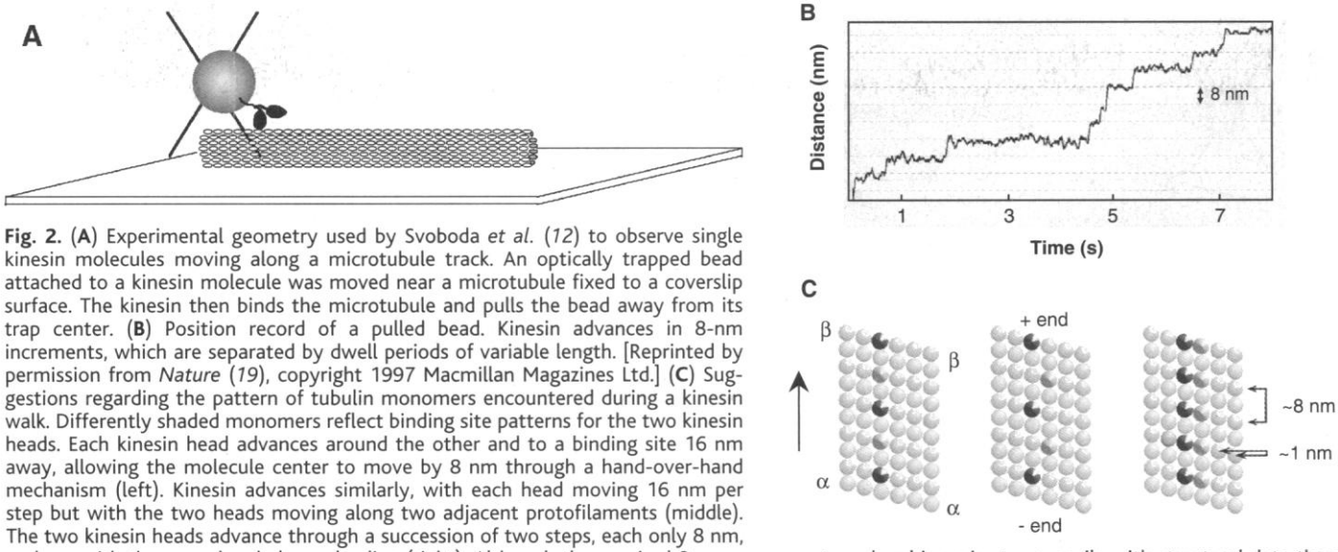

Fig. 2. (**A**) Experimental geometry used by Svoboda *et al.* (*12*) to observe single kinesin molecules moving along a microtubule track. An optically trapped bead attached to a kinesin molecule was moved near a microtubule fixed to a coverslip surface. The kinesin then binds the microtubule and pulls the bead away from its trap center. (**B**) Position record of a pulled bead. Kinesin advances in 8-nm increments, which are separated by dwell periods of variable length. [Reprinted by permission from *Nature* (*19*), copyright 1997 Macmillan Magazines Ltd.] (**C**) Suggestions regarding the pattern of tubulin monomers encountered during a kinesin walk. Differently shaded monomers reflect binding site patterns for the two kinesin heads. Each kinesin head advances around the other and to a binding site 16 nm away, allowing the molecule center to move by 8 nm through a hand-over-hand mechanism (left). Kinesin advances similarly, with each head moving 16 nm per step but with the two heads moving along two adjacent protofilaments (middle). The two kinesin heads advance through a succession of two steps, each only 8 nm, perhaps with the same head always leading (right). Although the required 8-nm movement per head is easier to reconcile with structural data than a 16-nm advance, this concerted sequence of two heads moving would need to occur with only one ATP bound to one head. [Reprinted by permission from *Cell* (*21*), copyright 1998 Cell Press.]

the actin filament axis. To better control protein orientation, Tanaka *et al.* (*38*) used a synthetic myosin cofilament, which was a mixture of single-headed myosin and myosin rod (the myosin tail without the head or neck). They found a mean bead displacement around 10 nm when the myosin and actin filaments were optimally aligned, near 0 nm when they were orthogonal, and (perhaps surprisingly) at 5 nm in the same actin filament direction when they were almost oppositely aligned. This suggests that measurements of randomly oriented myosin may underestimate the step size.

The term myosin refers to at least 14 classes of proteins, each containing putative or demonstrated actin-based motors and each likely filling different roles. The studies described so far all involve skeletal muscle myosin (myosin II), but other isoforms of myosin have also been investigated. Guilford *et al.* (*35*) demonstrated that the bound state dwell time for smooth muscle myosin is four to five times as long as that for skeletal myosin, under low- and high-load conditions. Thus, the higher isometric forces (forces generated under conditions that arrest movement by load) that are generated by smooth muscles may be caused by every given molecule sustaining force for a longer time [an idea supported by measured ADP release rates (*39*)]. Moreover, electron microscopy reconstruction studies of several myosin family members bound to actin indicate that smooth muscle myosin and others will move the actin by an additional several nanometers after releasing ADP and before binding ATP and detaching from the actin (*40, 41*). Future experiments should allow the direct observation of such added steps.

Ishijima *et al.* (*34*) recently expanded on the dumbbell experiment by observing simultaneously mechanical steps (Fig. 3B, top and middle traces) and fluorescent nucleotides through total internal reflection microscopy. They detected myosin attachment events by the increase in stiffness of elements constraining bead diffusion (Fig. 3B, middle trace), and they detected fluorescently labeled nucleotide arrival in the focal plane as an increase in the fluorescent intensity photon count (Fig. 3B, bottom trace). The results demonstrate one-to-one coupling between ATP turnover and the observed mechanical cycle of binding and releasing actin. Moreover, in a minority of cases, myosin appeared to release its nucleotide before binding and moving the actin filament. Ishijima *et al.* argue that this requires a "hysteretic" state of myosin, which somehow preserves the memory of and energy from a complete ATP turnover that occurred as long as half a second before binding the actin (*34*).

Models of the myosin-actin interaction predominantly invoke a conformational change in the myosin molecule that is tightly coupled to the hydrolysis of one ATP molecule, but less conventional views of the motor mechanism continue to have supporters. For instance, a "thermal ratchet" mechanism (*42*) or some other means for "loose" mechanochemical coupling (multiple mechanical steps per each hydrolyzed ATP) might predict that myosin would move along actin in a cluster of small steps. Evidence of such behavior has recently been presented by Kitamura *et al.* (*43*), who show with a microneedle technique that a myosin-products complex after a single

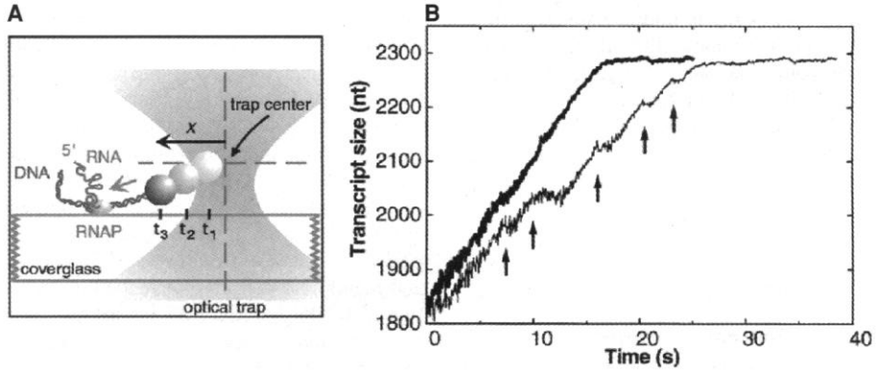

Fig. 4. (**A**) Experimental geometry used by Yin *et al.* (*53*) to observe single RNAP molecules pulling a DNA template. RNAP was fixed to a surface and allowed to bind solution DNA strands, which were attached to beads on their transcriptionally downstream ends. The beads were then trapped, and their displacements (x) were observed as time progressed from t_1 to t_3. [Reprinted from (*54*).] (**B**) After correcting for geometry and DNA elasticity, the movement of DNA through RNAP can be extracted from the bead position data. The bottom trace shows such movement, which was interrupted occasionally by apparent transcriptional pauses (marked by arrows). The top trace shows the same movement with pauses algorithmically removed, as needed to compute a meaningful transcription velocity. nt, nucleotides. [Reprinted from (*54*).]

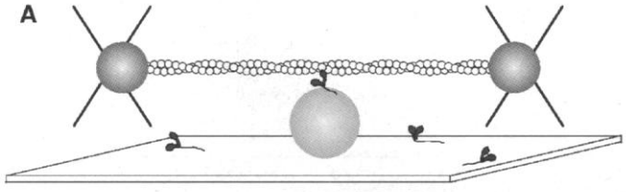

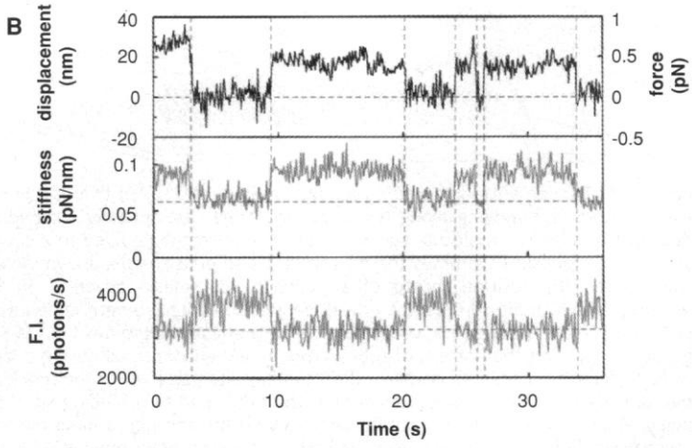

Fig. 3. (**A**) Experimental geometry used by Finer *et al.* (*32*) to observe single myosin molecules binding and pulling an actin filament. The filament is attached on either end to a trapped bead. These beads are used to stretch the filament taut and move it near surface-bound silica beads that were decorated sparsely with myosin molecules. [Reprinted by permission from *Nature* (*32*), copyright 1994 Macmillan Magazines Ltd.] (**B**) Data traces in which such mechanical experiments are combined with single-fluorophore detection to track fluorescently labeled ATPs that are associated with mechanical actomyosin interactions. The top trace shows bead displacement that is parallel to the long actin filament axis. The middle trace shows the stiffness of elements constraining bead diffusion, which is used as a signature to track myosin binding even if the bead is not substantially displaced. At the baseline, the traps alone constrain diffusion. When myosin binds, a stiff surface linkage increases this constraint. The bottom trace shows the fluorescence intensity (F.I.) photon count, which is used to observe single ATPs moving into and out of the focal plane. Myosin binding actin corresponds to nucleotide release, and myosin binding nucleotide corresponds to actin release. [Reprinted by permission from *Cell* (*34*), copyright 1998 Cell Press.]

ATP hydrolysis can interact with actin in a series of short-lasting 5.5-nm steps.

It is important to establish definitive values of the unitary displacement and force for myosin, as these values can help to distinguish between competing models of how the muscle works. The existence of substantial compliance between the actin filament and beads in the dumbbell system has complicated the issue by reducing the measured bead displacement and by preventing investigators from isometrically clamping the myosin molecule (*36, 37, 44*). The microneedle technique (*43, 45*) has proven to be superior in generating noncompliant linkages, but it is more onerous experimentally and less adaptable to rapid feedback control. Rigid links, defined protein orientations, and feedback systems [see (*46*)] should enable a host of single-molecule measurements that are analogous to seminal experiments with whole muscle fibers [see (*47*)], observing conformational change directly and perhaps arresting stable intermediates by applied load. Moreover, combination with fluorescent methods of detecting myosin shape changes and actin movements (*48–50*) should allow observation of how the molecular structure generates force or responds to applied force.

RNA Polymerase: A Processive DNA Transcription Machine

The enzyme RNA polymerase (RNAP) transcribes a DNA template into messenger RNA. In doing so, it draws energy from the nucleotide condensation reaction to drive movement along the DNA template (*51*). Schafer *et al.* (*52*) mounted RNAP molecules on a surface and allowed them to bind from solution DNA strands attached to beads at their transcriptionally downstream ends. The RNAP complex then pulls the bead toward the surface as it threads through the DNA template. Yin *et al.* (*53*) extended this experiment by trapping the bead (Fig. 4A).

In early work, Yin *et al.* (*53*) measured the stall force against which RNAP ceased to move, which is analogous to that described above for kinesin except that many stalled complexes did not resume movement when the load was reduced. Several molecules stalled against loads of 12.3 ± 3.5 pN, which was probably an underestimate because some complexes did not stall and some may have suffered laser light exposure damage. Wang *et al.* (*54*) introduced a feedback scheme to increase the effective trap strength while reducing light exposure; they determined a stall force of ~21 to 27 pN. All of these values exceed the 5 to 7 pN that were measured for kinesin, perhaps reflecting the need for RNAP to forcefully disentangle DNA secondary structure.

Wang *et al.* made appropriate elastic and geometric corrections to extract relative RNAP-DNA movements from the bead position data (Fig. 4B) (*55*), which allowed them to observe the transcription process more directly (*54*). They observed transient pauses for 0 to 30 s (Fig. 4B), a time that is comparable to the delay that occurs before a reversibly stalled complex resumes movement after load reduction. The pause times may reflect rate constants of transition from a nonproductive state of the catalytic site complex. Not all stalled complexes resumed movement.

Finally, Wang *et al.* (*54*) computed RNAP velocity as a function of resistive force. After averaging out or algorithmically removing transcriptional pauses from the data, the velocity remained fairly constant against variable load until it declined sharply near the stall force, suggesting that the rate-limiting process at low force is not load dependent and thus does not involve mechanical advance. From the profile of decreasing velocity against forces near stall, Wang *et al.* estimated that the strain involved in causing arrest spans a distance of 5 to 10 base pairs (*54*). This may indicate that movement between adjacent bases is arrested by conformational strain that is 5 to 10 times as large as the distance traversed (the base to base separation along the strand). Alternatively, stall may follow slippage by that distance in the transcriptionally upstream direction.

The RNAP step size has not yet been determined, but it is anticipated to be a single base-pair separation. Future experiments should not only confirm this but also examine the influences of specific DNA sequences or protein cofactors on RNAP activity. The technology developed to study RNAP should now be applied to a broad array of DNA-based proteins.

Polymer Elasticity and Domain Unfolding

Pioneering measurements of biopolymer elasticity employed optical tweezers and other mechanical probes to stretch DNA (*56–58*). Such experiments pulled biopolymers beyond their entropically determined regime where the polymer resists an extension that constrains its range of accessible conformations and into one where external forces disturb the structure and induce conformational changes (*57–60*). The forceful breakage of actin monomer-monomer links with microneedles (*61*) and the breakage of receptor-

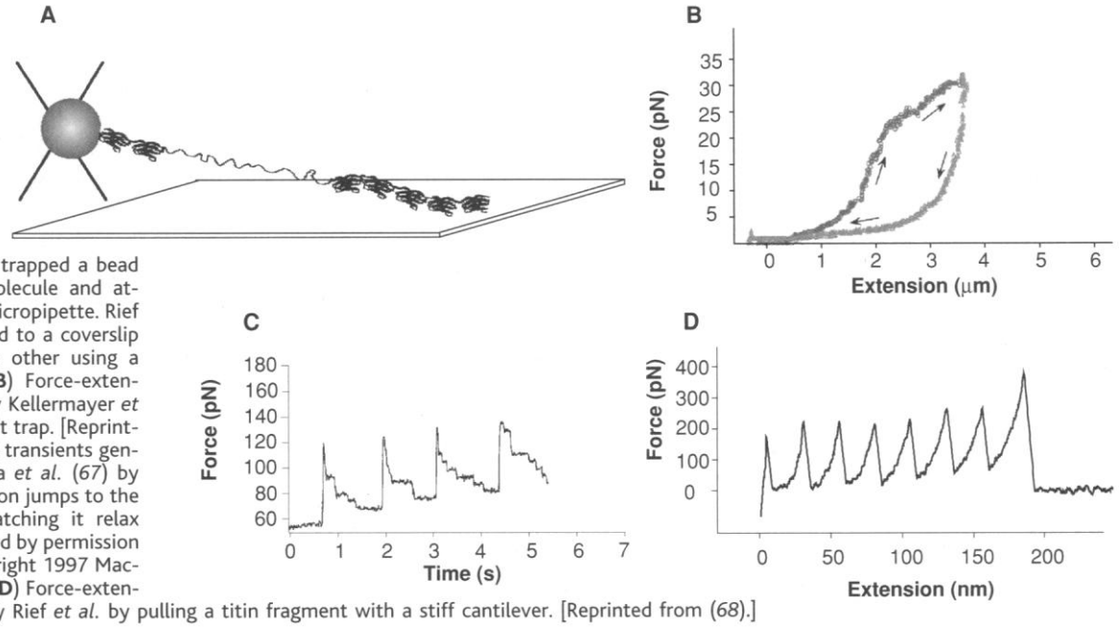

Fig. 5. (**A**) Experimental geometry used by Tskhovrebova *et al.* (*67*) to pull single titin molecules. A bead attached by an antibody to one end of a titin molecule was trapped and pulled; the other end was fixed to the microscope coverslip. Kellermayer *et al.* (*66*) trapped a bead on one end of the molecule and attached the other to a micropipette. Rief *et al.* (*68*) fixed one end to a coverslip surface and pulled the other using a stiff AFM cantilever. (**B**) Force-extension curve generated by Kellermayer *et al.* (*66*) with a compliant trap. [Reprinted from (*66*).] (**C**) Force transients generated by Tskhovrebova *et al.* (*67*) by applying transient tension jumps to the molecule and then watching it relax incrementally. [Reprinted by permission from *Nature* (*67*), copyright 1997 Macmillan Magazines Ltd.] (**D**) Force-extension curve generated by Rief *et al.* by pulling a titin fragment with a stiff cantilever. [Reprinted from (*68*).]

ligand links with AFMs (*62–65*) provided insights regarding the mechanical stability of biomolecular interactions. Here, we focus on recent experiments that used optical tweezers (Fig. 5A) (*66, 67*) and AFM cantilevers (*68*) to pull and reversibly unfold single immunoglobulin (Ig) and fibronectin III (Fn3) domains within the 3-MD muscle protein titin (*69*), which is responsible for the structural integrity and elasticity of relaxed muscle. This work encompassed both the polymer properties of the titin molecule and the forced unfolding of its domains.

Figure 5B shows a force-extension curve for a single titin molecule through a stretch and relax cycle (*66*). Titin has a flexible elastic segment of proline, glutamate, valine, and lysine (PEVK) (*70*), which is flanked by over 200 tandem Ig and Fn3 domains (*71*). Under low forces, long molecules like titin (~1 μm when extended) respond to force as described by standard polymer models of entropic chains. The force-extension relation below 30 pN can be dissected into two entropic components (*67*), corresponding to the straightening of the tandem Ig and Fn3 domains and the straightening of the PEVK segment, which is probably a random peptide coil. Under higher forces, titin experiences conformational change; the force-extension relation levels off above 30 pN (Fig. 5B) as a result of the sequential unfolding of Ig and Fn3 domains. The moving probe increases tension quickly (as compared to the unfolding rates), and therefore, the domains unfold at a higher force than they would under equilibrium measurements. During relaxation, the domains refold only at very low force because the domains must collect their polypeptide backbone into a small volume. Thus, after the reversal of probe movement direction, the force decreases to reflect the entropic elasticity of the unfolded domains.

In their optical trap experiment, Kellermayer *et al.* (*66*) (Fig. 5B) did not observe individual domain unfolding events but rather inferred them from changes in the steady-state force-extension curve. Tskhovrebova *et al.* (*67*) observed such events directly, also using an optical trap but with a different approach. After a sudden step in trap position and thus a jump in system tension, they observed a staircaselike decline in force, with each step corresponding to the unfolding of one or more domains (Fig. 5C). The unitary unfolding events are more visible in the AFM force-extension traces (in Fig. 5D, as compared to Fig. 5B) recorded by Rief *et al.* (*68*), because a higher probe stiffness allows for a larger decline in force as each domain unfolded. When pulling an eight-domain Ig fragment with a stiff cantilever, they observed a sawtooth force-extension pattern punctuated by large declines in force. In a recent study, Rief *et al.* (*72*) demonstrated that the length change upon domain unfolding could be mapped to the unfolded length of the domains with single amino acid precision.

Applied force perturbs the equilibrium between the unfolded and folded state. The unfolding rate constant should depend exponentially on the applied force (*73, 74*), and the probability of unfolding depends on both the rate constant and the time allowed. If the pulling velocities are different, the measured unfolding forces will differ even if the rate constants are identical. Rief *et al.* (*72, 75*) showed that the different unfolding forces observed in Fig. 5 may be accounted for simply by the different stretching speeds used.

An interesting aspect of these studies concerns the highly cooperative manner in which the domains break. Corroborating this, recent molecular dynamics simulations (*76*) show that the forced unfolding is an all-or-none event, lacking stable intermediates. Disruption is dominated by kinetics (in particular, the disruption of the first few hydrogen bonds). Whether mechanical unfolding and thermally or denaturant-induced unfolding occur by the same pathway remains to be seen. It appears that β structures in the Ig domains in titin or in the Fn3 domains in titin and tenascin (*72, 77*) unfold at higher forces than do α-helical structures, at least in spectrin repeats, when they are stretched at the same speed (*78*). In contrast, thermal unfolding experiments had shown that domains composed of the two secondary structure types had comparable stability (*79, 80*).

The initial studies in this field have concentrated on a relatively few native structural motifs. However, there is much to be gained from studies of other motifs and of mutated structures.

Conclusions

Many challenges for single-molecule study with optical methods are now biological rather than technological and include the following examples: how to couple, say, ribosome or helicase activity to trapped bead motion; how to define and control molecular alignment; and how to mount proteins as to preserve function and minimize linkage compliance. Even in the case of well-studied proteins such as myosin, kinesin, and titin, mutational and biochemical studies continue to outpace single-molecule measurements. The coming years should see a productive merger of mutational techniques and single-molecule observations, which would elucidate structure-function relations with increasing precision. Such studies should spill over into clinically relevant areas (for instance, in cases of human mutant myosins that are implicated in familial hypertrophic cardiomyopathy and inherited deafness and blindness). Moreover, the proteins described here have numerous relatives awaiting study; the myosin family includes at least 14 unique classes, and many of these have been identified only through gene sequence homology. Expressing such proteins and measuring their mechanical properties should help elucidate their functions and no doubt produce a few surprises. Along with these developments, fluorescent methods [see (*81*)] will be combined with mechanical ones, allowing mechanical and kinetic characterization of single-protein shape changes and the movements or forces that they generate.

References

1. M. P. Sheetz, Ed., *Laser Tweezers in Cell Biology*, vol. 55 of *Methods in Cell Biology* (Academic Press, New York, 1997).
2. S. M. Block, D. F. Blair, H. C. Berg, *Nature* **338**, 514 (1989).
3. H. Noji, R. Yasuda, M. Yoshida, K. Kinosita Jr., *ibid.* **386**, 299 (1997).
4. K. Kinosita Jr., R. Yasuda, H. Noji, S. Ishiwata, M. Yoshida, *Cell* **93**, 21 (1998).
5. P. D. Boyer, *Annu. Rev. Biochem.* **66**, 717 (1997).
6. R. Yasuda, H. Noji, K. Kinosita Jr., M. Yoshida, *Cell* **93**, 1117 (1998).
7. J. Howard, *Nature* **389**, 561 (1997).
8. T. M. Lohman, K. Thorn, R. D. Vale, *Cell* **93**, 9 (1998).
9. J. Howard, A. J. Hudspeth, R. D. Vale, *Nature* **342**, 154 (1989).
10. S. M. Block, L. S. Goldstein, B. J. Schnapp, *ibid.* **348**, 348 (1990).
11. R. D. Vale *et al.*, *ibid.* **380**, 451 (1996).
12. K. Svoboda, C. F. Schmidt, B. J. Schnapp, S. M. Block, *ibid.* **365**, 721 (1993).
13. H. Kojima, E. Muto, H. Higuchi, T. Yanagida, *Biophys J.* **73**, 2012 (1997).
14. C. M. Coppin, D. W. Pierce, L. Hsu, R. D. Vale, *Proc. Natl. Acad. Sci. U.S.A.* **94**, 8539 (1997).
15. K. Svoboda and S. M. Block, *Cell* **77**, 773 (1994).
16. E. Meyhofer and J. Howard, *Proc. Natl. Acad. Sci. U.S.A.* **92**, 574 (1995).
17. M. J. Schnitzer and S. M. Block, *Cold Spring Harbor Symp. Quant. Biol.* **60**, 793 (1995).
18. W. Hua, E. C. Young, M. L. Fleming, J. Gelles, *Nature* **388**, 390 (1997).
19. M. J. Schnitzer and S. M. Block, *ibid.*, p. 386.
20. K. Svoboda, P. P. Mitra, S. M. Block, *Proc. Natl. Acad. Sci. U.S.A.* **91**, 11782 (1994).
21. S. M. Block, *Cell* **93**, 5 (1998).
22. F. Kozielski *et al.*, *ibid.* **91**, 985 (1997).
23. L. Romberg, D. W. Pierce, R. D. Vale, *J. Cell Biol.* **140**, 1407 (1998).
24. E. Berliner, E. C. Young, K. Anderson, H. K. Mahtani, J. Gelles, *Nature* **373**, 718 (1995).
25. Y. Inoue *et al.*, *Proc. Natl. Acad. Sci. U.S.A.* **94**, 7275 (1997).
26. E. C. Young, H. K. Mahtani, J. Gelles, *Biochemistry* **37**, 3467 (1998).
27. W. O. Hancock and J. Howard, *J. Cell Biol.* **140**, 1395 (1998).
28. K. Visscher and S. M. Block, *Methods Enzymol.* **298**, 460 (1998).
29. J. A. Spudich, *Cell Regul.* **1**, 1 (1989).
30. F. J. Kull, E. P. Sablin, R. Lau, R. J. Fletterick, R. D. Vale, *Nature* **380**, 550 (1996).
31. J. A. Spudich, *ibid.* **372**, 515 (1994).
32. J. T. Finer, R. M. Simmons, J. A. Spudich, *ibid.* **368**, 113 (1994).
33. J. E. Molloy, J. E. Burns, J. Kendrick-Jones, R. T. Tregear, D. C. White, *ibid.* **378**, 209 (1995).
34. A. Ishijima *et al.*, *Cell* **92**, 161 (1998).
35. W. H. Guilford *et al.*, *Biophys J.* **72**, 1006 (1997).
36. A. D. Mehta, J. T. Finer, J. A. Spudich, *Proc. Natl. Acad. Sci. U.S.A.* **94**, 7927 (1997).
37. C. Veigel, M. L. Bartoo, D. C. White, J. C. Sparrow, J. E. Molloy, *Biophys. J.* **75**, 1424 (1998).
38. H. Tanaka, A. Ishijima, M. Honda, K. Saito, T. Yanagida, *ibid.*, p. 1886.

39. C. R. Cremo and M. A. Geeves, *Biochemistry* **37**, 1969 (1998).
40. M. Whittaker *et al.*, *Nature* **378**, 748 (1995).
41. J. D. Jontes, E. M. Wilson-Kubalek, R. A. Milligan, *ibid.*, p. 751.
42. R. D. Astumian, *Science* **276**, 917 (1997).
43. K. Kitamura, M. Tokunaga, A. H. Iwane, T. Yanagida, *Nature* **397**, 129 (1999).
44. D. E. Dupuis, W. H. Guilford, J. Wu, D. M. Warshaw, *J. Muscle Res. Cell Motil.* **18**, 17 (1997).
45. A. Ishijima *et al.*, *Biophys. J.* **70**, 383 (1996).
46. R. M. Simmons, J. T. Finer, S. Chu, J. A. Spudich, *ibid.*, p. 1813.
47. A. F. Huxley and R. M. Simmons, *Nature* **233**, 533 (1971).
48. T. Funatsu, Y. Harada, M. Tokunaga, K. Saito, T. Yanagida, *ibid.* **374**, 555 (1995).
49. D. M. Warshaw *et al.*, *Proc. Natl. Acad. Sci. U.S.A.* **95**, 8034 (1998).
50. Y. Suzuki, T. Yasunaga, R. Ohkura, T. Wakabayashi, K. Sutoh, *Nature* **396**, 380 (1998).
51. J. Gelles and R. Landick, *Cell* **93**, 13 (1998).
52. D. A. Schafer, J. Gelles, M. P. Sheetz, R. Landick, *Nature* **353**, 444 (1991).
53. H. Yin *et al.*, Science **270**, 1653 (1995).
54. M. D. Wang *et al.*, *ibid.* **282**, 902 (1998).
55. M. D. Wang, H. Yin, R. Landick, J. Gelles, S. M. Block, *Biophys. J.* **72**, 1335 (1997).
56. S. B. Smith, L. Finzi, C. Bustamante, *Science* **258**, 1122 (1992).
57. S. B. Smith, Y. Cui, C. Bustamante, *ibid.* **271**, 795 (1996).
58. P. Cluzel *et al.*, *ibid.*, p. 792.
59. M. Rief, F. Oesterhelt, B. Heymann, H. E. Gaub, *ibid.* **275**, 1295 (1997).
60. P. E. Marszalek, A. F. Oberhauser, Y. P. Pang, J. M. Fernandez, *Nature* **396**, 661 (1998).
61. A. Kishino and T. Yanagida, *ibid.* **334**, 74 (1988).
62. E.-L. Florin, V. T. Moy, H. E. Gaub, *Science* **264**, 415 (1994).
63. G. U. Lee, D. A. Kidwell, R. J. Colton, *Langmuir* **10**, 354 (1994).
64. P. Hinterdorfer, W. Baumgartner, H. J. Gruber, K. Schilcher, H. Schindler, *Proc. Natl. Acad. Sci. U.S.A.* **93**, 3477 (1996).
65. U. Dammer *et al.*, *Biophys. J.* **70**, 2437 (1995).
66. M. S. Z. Kellermayer, S. B. Smith, H. L. Granzier, C. Bustamante, *Science* **276**, 1112 (1997).
67. L. Tskhovrebova, J. Trinick, J. A. Sleep, R. M. Simmons, *Nature* **387**, 308 (1997).
68. M. Rief, M. Gautel, F. Oesterhelt, J. M. Fernandez, H. E. Gaub, *Science* **276**, 1109 (1997).
69. K. Maruyama *et al.*, *J. Biochem. Tokyo* **82**, 317 (1977).
70. M. Gautel and D. Goulding, *FEBS Lett.* **385**, 11 (1996).
71. S. Labeit and B. Kolmerer, *Science* **270**, 293 (1995).
72. M. Rief, M. Gautel, A. Schemmel, H. E. Gaub, *Biophys. J.* **75**, 3008 (1998).
73. G. I. Bell, *Science* **200**, 618 (1978).
74. E. Evans and K. Ritchie, *Biophys. J.* **72**, 1541 (1997).
75. M. Rief, J. M. Fernandez, H. E. Gaub, *Phys. Rev. Lett.* **81**, 4764 (1998).
76. H. Lu, B. Isralewitz, A. Krammer, V. Vogel, K. Schulten, *Biophys. J.* **75**, 662 (1998).
77. A. F. Oberhauser, P. E. Marszalek, H. P. Erickson, J. M. Fernandez, *Nature* **393**, 181 (1998).
78. M. Rief, J. Pascual, M. Saraste, H. E. Gaub, *J. Mol. Biol.* **286**, 553 (1999).
79. T. M. DeSilva *et al.*, *Biochemistry* **36**, 3991 (1997).
80. A. S. Politou, D. J. Thomas, A. Pastore, *Biophys. J.* **69**, 2601 (1995).
81. S. Weiss, *Science* **283**, 1676 (1999).